Received 24 September; accepted 16 November 2004; doi:10.1038/nature03211.

1. MacArthur, R. H. & Wilson, E. O. *The Theory of Island Biogeography* (Princeton Univ. Press, Princeton, 1969).
2. Fisher, R. A., Corbet, A. S. & Williams, C. B. The relation between the number of species and the number of individuals in a random sample of an animal population. *J. Anim. Ecol.* **12,** 42–58 (1943).
3. Preston, F. W. The commonness, and rarity, of species. *Ecology* **41,** 611–627 (1948).
4. Brown, J. H. *Macroecology* (Univ. Chicago Press, Chicago, 1995).
5. Hubbell, S. P. A unified theory of biogeography and relative species abundance and its application to tropical rain forests and coral reefs. *Coral Reefs* **16,** S9–S21 (1997).
6. Hubbell, S. P. *The Unified Theory of Biodiversity and Biogeography* (Princeton Univ. Press, Princeton, 2001).
7. Caswell, H. Community structure: a neutral model analysis. *Ecol. Monogr.* **46,** 327–354 (1976).
8. Bell, G. Neutral macroecology. *Science* **293,** 2413–2418 (2001).
9. Elton, C. S. *Animal Ecology* (Sidgwick and Jackson, London, 1927).
10. Gause, G. F. *The Struggle for Existence* (Hafner, New York, 1934).
11. Hutchinson, G. E. Homage to Santa Rosalia or why are there so many kinds of animals? *Am. Nat.* **93,** 145–159 (1959).
12. Huffaker, C. B. Experimental studies on predation: dispersion factors and predator-prey oscillations. *Hilgardia* **27,** 343–383 (1958).
13. Paine, R. T. Food web complexity and species diversity. *Am. Nat.* **100,** 65–75 (1966).
14. MacArthur, R. H. *Geographical Ecology* (Harper & Row, New York, 1972).
15. Laska, M. S. & Wootton, J. T. Theoretical concepts and empirical approaches to measuring interaction strength. *Ecology* **79,** 461–476 (1998).
16. McGill, B. J. Strong and weak tests of macroecological theory. *Oikos* **102,** 679–685 (2003).
17. Adler, P. B. Neutral models fail to reproduce observed species-area and species-time relationships in Kansas grasslands. *Ecology* **85,** 1265–1272 (2004).
18. Connell, J. H. The influence of interspecific competition and other factors on the distribution of the barnacle *Chthamalus stellatus*. *Ecology* **42,** 710–723 (1961).
19. Paine, R. T. Ecological determinism in the competition for space. *Ecology* **65,** 1339–1348 (1984).
20. Wootton, J. T. Prediction in complex communities: analysis of empirically-derived Markov models. *Ecology* **82,** 580–598 (2001).
21. Wootton, J. T. Markov chain models predict the consequences of experimental extinctions. *Ecol. Lett.* **7,** 653–660 (2004).
22. Paine, R. T. Food-web analysis through field measurements of per capita interaction strength. *Nature* **355,** 73–75 (1992).
23. Moore, J. C., de Ruiter, P. C. & Hunt, H. W. The influence of productivity on the stability of real and model ecosystems. *Science* **261,** 906–908 (1993).
24. Rafaelli, D. G. & Hall, S. J. in *Food Webs: Integration of Pattern and Dynamics* (eds Polis, G. & Winemiller, K.) 185–191 (Chapman and Hall, New York, 1996).
25. Wootton, J. T. Estimates and tests of per-capita interaction strength: diet, abundance, and impact of intertidally foraging birds. *Ecol. Monogr.* **67,** 45–64 (1997).
26. Kokkoris, G. D., Troumbis, A. Y. & Lawton, J. H. Patterns of species interaction strength in assembled theoretical competition communities. *Ecol. Lett.* **2,** 70–74 (1999).
27. Drossel, B., McKane, A. & Quince, C. The impact of nonlinear functional responses on the long-term evolution of food web structure. *J. Theor. Biol.* **229,** 539–548 (2004).

Acknowledgements I thank the Makah Tribal Council for providing access to Tatoosh Island; J. Sheridan, J. Salamunovitch, F. Stevens, A. Miller, B. Scott, J. Chase, J. Shurin, K. Rose, L. Weis, R. Kordas, K. Edwards, M. Novak, J. Duke, J. Orcutt, K. Barnes, C. Neufeld and L. Weintraub for field assistance; and NSF, EPA (CISES) and the Andrew W. Mellon foundation for partial financial support.

Competing interests statement The author declares that he has no competing financial interests.

Correspondence and requests for materials should be addressed to J.T.W. (twootton@uchicago.edu).

Evolutionary dynamics on graphs

Erez Lieberman[1,2], Christoph Hauert[1,3] & Martin A. Nowak[1]

[1]*Program for Evolutionary Dynamics, Departments of Organismic and Evolutionary Biology, Mathematics, and Applied Mathematics, Harvard University, Cambridge, Massachusetts 02138, USA*
[2]*Harvard-MIT Division of Health Sciences and Technology, Massachusetts Institute of Technology, Cambridge, Massachusetts, USA*
[3]*Department of Zoology, University of British Columbia, Vancouver, British Columbia V6T 1Z4, Canada*

Evolutionary dynamics have been traditionally studied in the context of homogeneous or spatially extended populations[1–4]. Here we generalize population structure by arranging individuals on a graph. Each vertex represents an individual. The weighted edges denote reproductive rates which govern how often individuals place offspring into adjacent vertices. The homogeneous population, described by the Moran process[3], is the special case of a fully connected graph with evenly weighted edges. Spatial structures are described by graphs where vertices are connected with their nearest neighbours. We also explore evolution on random and scale-free networks[5–7]. We determine the fixation probability of mutants, and characterize those graphs for which fixation behaviour is identical to that of a homogeneous population[7]. Furthermore, some graphs act as suppressors and others as amplifiers of selection. It is even possible to find graphs that guarantee the fixation of any advantageous mutant. We also study frequency-dependent selection and show that the outcome of evolutionary games can depend entirely on the structure of the underlying graph. Evolutionary graph theory has many fascinating applications ranging from ecology to multi-cellular organization and economics.

Evolutionary dynamics act on populations. Neither genes, nor cells, nor individuals evolve; only populations evolve. In small populations, random drift dominates, whereas large populations

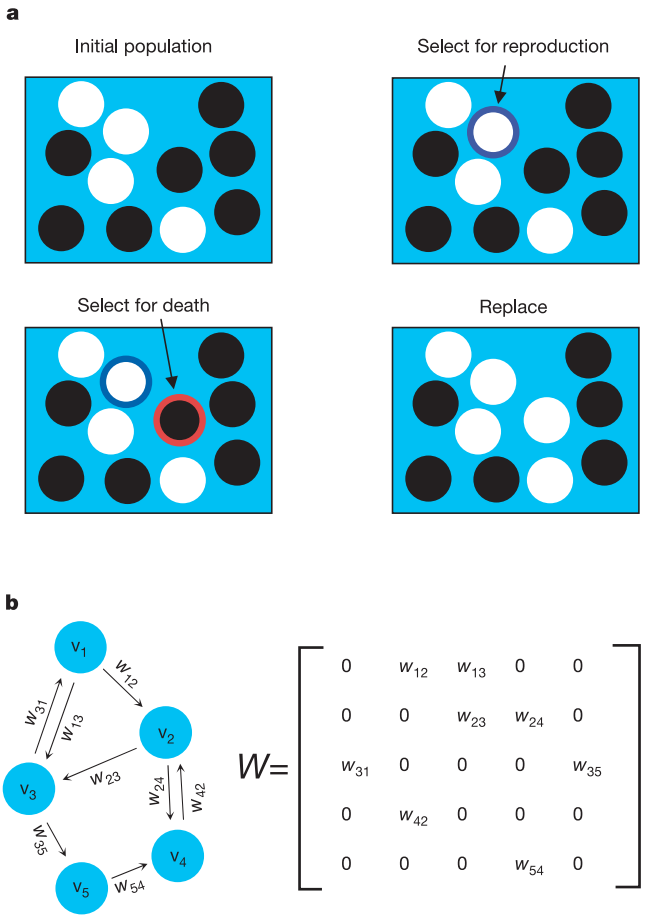

Figure 1 Models of evolution. **a**, The Moran process describes stochastic evolution of a finite population of constant size. In each time step, an individual is chosen for reproduction with a probability proportional to its fitness; a second individual is chosen for death. The offspring of the first individual replaces the second. **b**, In the setting of evolutionary graph theory, individuals occupy the vertices of a graph. In each time step, an individual is selected with a probability proportional to its fitness; the weights of the outgoing edges determine the probabilities that the corresponding neighbour will be replaced by the offspring. The process is described by a stochastic matrix W, where w_{ij} denotes the probability that an offspring of individual i will replace individual j. In a more general setting, at each time step, an edge ij is selected with a probability proportional to its weight and the fitness of the individual at its tail. The Moran process is the special case of a complete graph with identical weights.

are sensitive to subtle differences in selective values. The tension between selection and drift lies at the heart of the famous dispute between Fisher and Wright[8–10]. There is evidence that population structure affects the interplay of these forces[11–15]. But the celebrated results of Maruyama[16] and Slatkin[17] indicate that spatial structures are irrelevant for evolution under constant selection.

Here we introduce evolutionary graph theory, which suggests a promising new lead in the effort to provide a general account of how population structure affects evolutionary dynamics. We study the simplest possible question: what is the probability that a newly introduced mutant generates a lineage that takes over the whole population? This fixation probability determines the rate of evolution, which is the product of population size, mutation rate and fixation probability. The higher the correlation between the mutant's fitness and its probability of fixation, ρ, the stronger the effect of natural selection; if fixation is largely independent of fitness, drift dominates. We will show that some graphs are governed entirely by random drift, whereas others are immune to drift and are guided exclusively by natural selection.

Consider a homogeneous population of size N. At each time step an individual is chosen for reproduction with a probability proportional to its fitness. The offspring replaces a randomly chosen individual. In this so-called Moran process (Fig. 1a), the population size remains constant. Suppose all the resident individuals are identical and one new mutant is introduced. The new mutant has relative fitness r, as compared to the residents, whose fitness is 1. The fixation probability of the new mutant is:

$$\rho_1 = \frac{1 - 1/r}{1 - 1/r^N} \qquad (1)$$

This represents a specific balance between selection and drift: advantageous mutations have a certain chance—but no guarantee—of fixation, whereas disadvantageous mutants are likely—but again, no guarantee—to become extinct.

We introduce population structure as follows. Individuals are labelled $i = 1, 2, \ldots N$. The probability that individual i places its offspring into position j is given by w_{ij}.

Thus the individuals can be thought of as occupying the vertices of a graph. The matrix $W = [w_{ij}]$ determines the structure of the graph (Fig. 1b). If $w_{ij} = 0$ and $w_{ji} = 0$ then the vertices i and j are not connected. In each iteration, an individual i is chosen for reproduction with a probability proportional to its fitness. The resulting offspring will occupy vertex j with probability w_{ij}. Note that W is a stochastic matrix, which means that all its rows sum to one. We want to calculate the fixation probability ρ of a randomly placed mutant.

Imagine that the individuals are arranged on a spatial lattice that can be triangular, square, hexagonal or any similar tiling. For all such lattices ρ remains unchanged: it is equal to the ρ_1 obtained for the homogeneous population. In fact, it can be shown that if W is symmetric, $w_{ij} = w_{ji}$, then the fixation probability is always ρ_1. The graphs in Fig. 2a–c, and all other symmetric, spatially extended models, have the same fixation probability as a homogeneous population[17,18].

There is an even wider class of graphs whose fixation probability is ρ_1. Let $T_i = \Sigma_j w_{ji}$ be the temperature of vertex i. A vertex is 'hot' if it is replaced often and 'cold' if it is replaced rarely. The 'isothermal theorem' states that an evolutionary graph has fixation probability ρ_1 if and only if all vertices have the same temperature. Figure 2d gives an example of an isothermal graph where W is not symmetric. Isothermality is equivalent to the requirement that W is doubly stochastic, which means that each row and each column sums to one.

If a graph is not isothermal, the fixation probability is not given

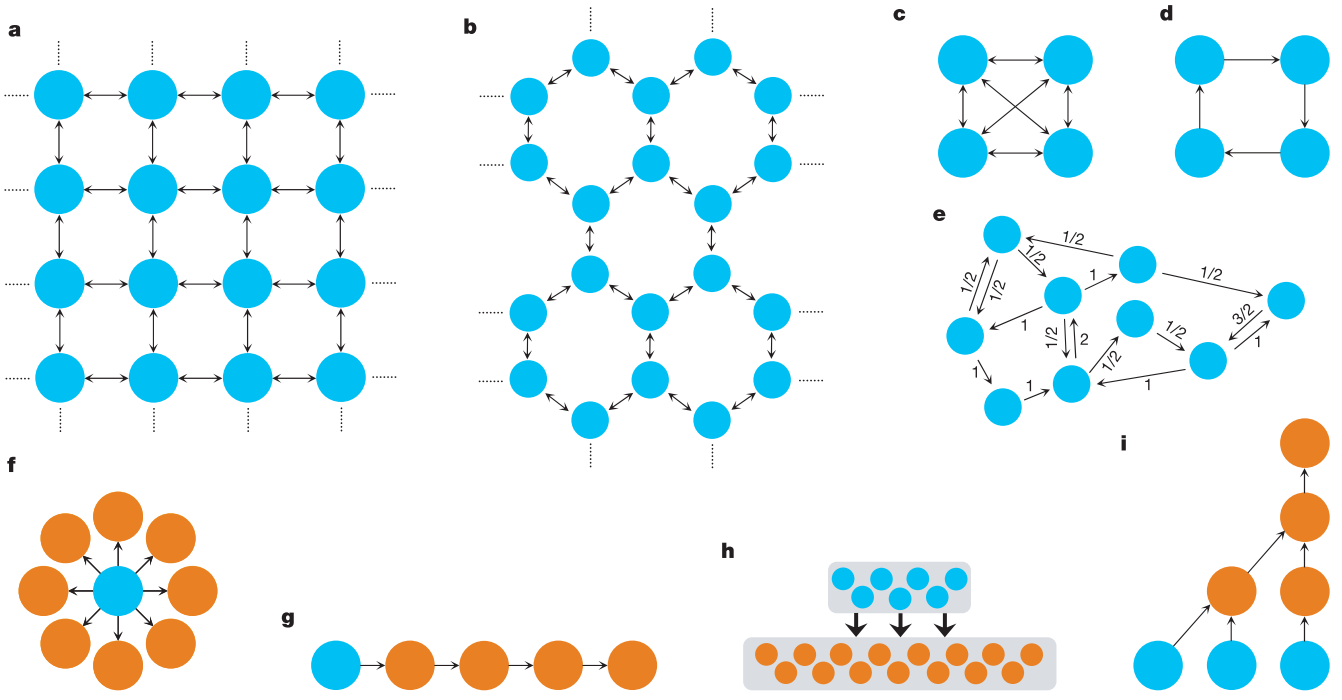

Figure 2 Isothermal graphs, and, more generally, circulations, have fixation behaviour identical to the Moran process. Examples of such graphs include: **a**, the square lattice; **b**, hexagonal lattice; **c**, complete graph; **d**, directed cycle; and **e**, a more irregular circulation. Whenever the weights of edges are not shown, a weight of one is distributed evenly across all those edges emerging from a given vertex. Graphs like **f**, the 'burst', and **g**, the 'path', suppress natural selection. The 'cold' upstream vertex is represented in blue. The 'hot' downstream vertices, which change often, are coloured in orange. The type of the upstream root determines the fate of the entire graph. **h**, Small upstream populations with large downstream populations yield suppressors. **i**, In multirooted graphs, the roots compete indefinitely for the population. If a mutant arises in a root then neither fixation nor extinction is possible.

by ρ_1. Instead, the balance between selection and drift tilts; now to one side, now to the other. Suppose N individuals are arranged in a linear array. Each individual places its offspring into the position immediately to its right. The leftmost individual is never replaced. What is the fixation probability of a randomly placed mutant with fitness r? Clearly, it is $1/N$, irrespective of r. The mutant can only reach fixation if it arises in the leftmost position, which happens with probability $1/N$. This array is an example of a simple population structure whose behaviour is dominated by random drift.

More generally, an evolutionary graph has fixation probability $1/N$ for all r if and only if it is one-rooted (Fig. 2f, g). A one-rooted graph has a unique global source without incoming edges. If a graph has more than one root, then the probability of fixation is always zero: a mutant originating in one of the roots will generate a lineage which will never die out, but also never fixate (Fig. 2i). Small upstream populations feeding into large downstream populations are also suppressors of selection (Fig. 2h). Thus, it is easy to construct graphs that foster drift and suppress selection. Is it possible to suppress drift and amplify selection? Can we find structures where the fixation probability of advantageous mutants exceeds ρ_1?

The star structure (Fig. 3a) consists of a centre that is connected with each vertex on the periphery. All the peripheral vertices are connected only with the centre. For large N, the fixation probability of a randomly placed mutant on the star is $\rho_2 = (1 - 1/r^2)/(1 - 1/r^{2N})$. Thus, any selective difference r is amplified to r^2. The star acts as evolutionary amplifier, favouring advantageous mutants and inhibiting disadvantageous mutants. The balance tilts towards selection, and against drift.

The super-star, funnel and metafunnel (Fig. 3) have the amazing property that for large N, the fixation probability of any advantageous mutant converges to one, while the fixation probability of any disadvantageous mutant converges to zero. Hence, these population structures guarantee fixation of advantageous mutants however small their selective advantage. In general, we can prove that for sufficiently large population size N, a super-star of parameter K satisfies:

$$\rho_K = \frac{1 - 1/r^K}{1 - 1/r^{KN}} \qquad (2)$$

Numerical simulations illustrating equation (2) are shown in Fig. 4a. Similar results hold for the funnel and metafunnel. Just as one-rooted structures entirely suppress the effects of selection, super-star structures function as arbitrarily strong amplifiers of selection and suppressors of random drift.

Scale-free networks, like the amplifier structures in Fig. 3, have most of their connectivity clustered in a few vertices. Such networks are potent selection amplifiers for mildly advantageous mutants (r

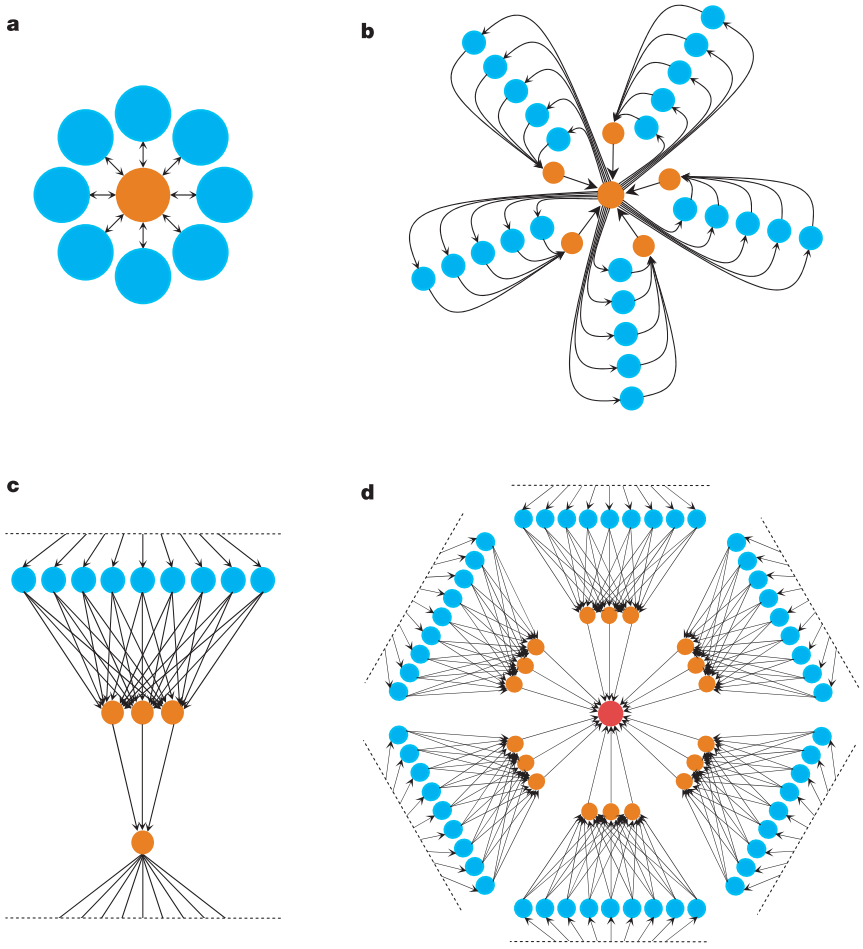

Figure 3 Selection amplifiers have remarkable symmetry properties. As the number of 'leaves' and the number of vertices in each leaf grows large, these amplifiers dramatically increase the apparent fitness of advantageous mutants: a mutant with fitness r on an amplifier of parameter K will fare as well as a mutant of fitness r^K in the Moran process. **a**, The star structure is a $K = 2$ amplifier. **b**–**d**, The super-star (**b**), the funnel (**c**) and the metafunnel (**d**) can all be extended to arbitrarily large K, thereby guaranteeing the fixation of any advantageous mutant. The latter three structures are shown here for $K = 3$. The funnel has edges wrapping around from bottom to top. The metafunnel has outermost edges arising from the central vertex (only partially shown). The colours red, orange and blue indicate hot, warm and cold vertices.

close to 1), and relax to ρ_1 for very advantageous mutants ($r \gg 1$) (Fig. 4b).

Further generalizations of evolutionary graphs are possible. Suppose in each iteration an edge ij is chosen with a probability proportional to the product of its weight, w_{ij}, and the fitness of the individual i at its tail. In this case, the matrix W need not be stochastic; the weights can be any collection of non-negative real numbers.

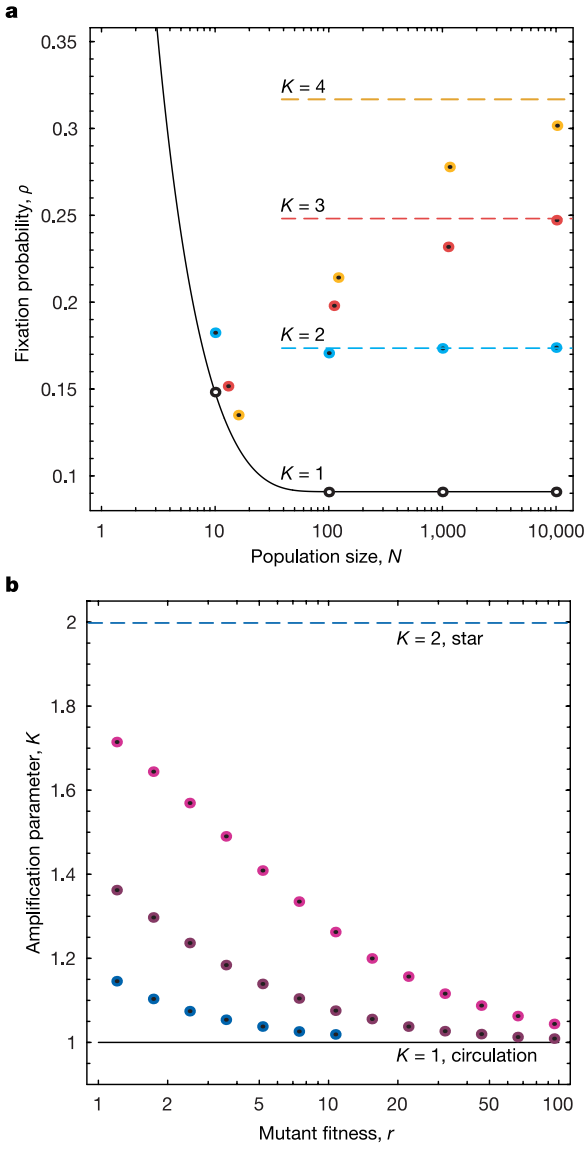

Figure 4 Simulation results showing the likelihood of mutant fixation. **a**, Fixation probabilities for an $r = 1.1$ mutant on a circulation (black), a star (blue), a $K = 3$ super-star (red), and a $K = 4$ super-star (yellow) for varying population sizes N. Simulation results are indicated by points. As expected, for large population sizes, the simulation results converge to the theoretical predictions (broken lines) obtained using equation (2). **b**, The amplification factor K of scale-free graphs with 100 vertices and an average connectivity of $2m$ with $m = 1$ (violet), $m = 2$ (purple), or $m = 3$ (navy) is compared to that for the star (blue line) and for circulations (black line). Increasing m increases the number of highly connected hubs. Scale-free graphs do not behave uniformly across the mutant spectrum: as the fitness r increases, the amplification factor relaxes from nearly 2 (the value for the star) to circulation-like values of unity. All simulations are based on 10^4–10^6 runs. Simulations can be explored online at http://www.univie.ac.at/virtuallabs/.

Here the results have a particularly elegant form. In the absence of upstream populations, if the sum of the weights of all edges leaving the vertex is the same for all vertices—meaning the fertility is independent of position—then the graph never suppresses selection. If the sum of the weights of all edges entering a vertex is the same for all vertices—meaning the mortality is independent of position—then the graph never suppresses drift. If both these conditions hold then the graph is called a circulation, and the structure favours neither selection nor drift. An evolutionary graph has fixation probability ρ_1 if and only if it is a circulation (see Fig. 2e). It is striking that the notion of a circulation, so common in deterministic contexts such as the study of flows, arises naturally in this stochastic evolutionary setting. The circulation criterion completely classifies all graph structures whose fixation behaviour is identical to that of the homogeneous population, and includes the subset of isothermal graphs (the mathematical details of these results are discussed in the Supplementary Information).

Let us now turn to evolutionary games on graphs[18,19]. Consider, as before, two types A and B, but instead of having constant fitness, their relative fitness depends on the outcome of a game with payoff matrix:

$$\begin{array}{c} \\ A \\ B \end{array} \begin{array}{c} \begin{array}{cc} A & B \end{array} \\ \begin{pmatrix} a & b \\ c & d \end{pmatrix} \end{array}$$

In traditional evolutionary game dynamics, a mutant strategy A can invade a resident B if $b > d$. For games on graphs, the crucial condition for A invading B, and hence the very notion of evolutionary stability, can be quite different.

As an illustration, imagine N players arranged on a directed cycle

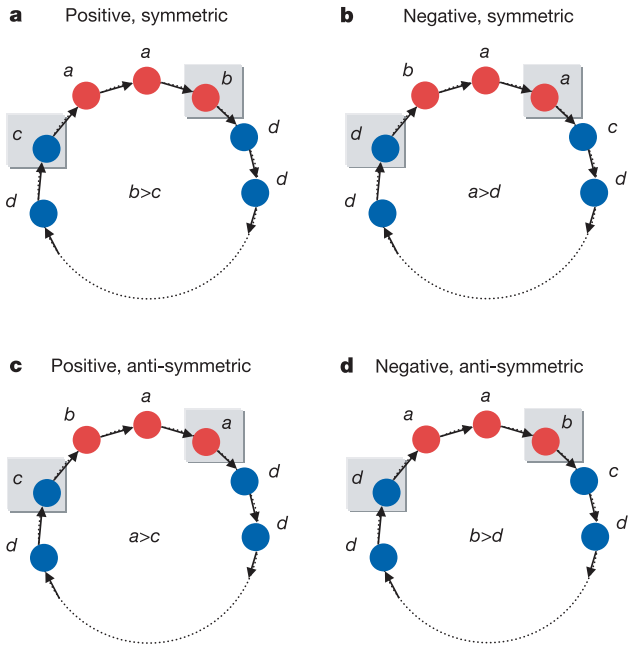

Figure 5 Evolutionary games on directed cycles for four different orientations. **a**, Positive symmetric. The invading mutant (red) is favoured over the resident (blue) if $b > c$. **b**, Negative symmetric. Invasion is favoured if $a > d$. For the Prisoner's Dilemma, the implication is that unconditional cooperators can invade and replace defectors starting from a single individual. **c**, Positive anti-symmetric. Invasion is favoured if $a > c$. The tables are turned: the invader behaves like a resident in a traditional setting. **d**, Negative anti-symmetric. Invasion is favoured if $b > d$. We recover the traditional invasion of evolutionary game theory.

(Fig. 5) with player i placing its offspring into $i+1$. In the simplest case, the payoff of any individual comes from an interaction with one of its neighbours. There are four natural orientations. We discuss the fixation probability of a single A mutant for large N.

(1) Positive symmetric: i interacts with $i+1$. The fixation probability is given by equation (1) with $r = b/c$. Selection favours the mutant if $b > c$.

(2) Negative symmetric: i interacts with $i-1$. Selection favours the mutant if $a > d$. In the classical Prisoner's Dilemma, these dynamics favour unconditional cooperators invading defectors.

(3) Positive anti-symmetric: mutants at i interact with $i-1$, but residents with $i+1$. The mutant is favoured if $a > c$, behaving like a resident in the classical setting.

(4) Negative anti-symmetric: Mutants at i interact with $i+1$, but residents with $i-1$. The mutant is favoured if $b > d$, recovering the traditional invasion criterion.

Remarkably, games on directed cycles yield the complete range of pairwise conditions in determining whether selection favours the mutant or the resident.

Circulations no longer behave identically with respect to games. Outcomes depend on the graph, the game and the orientation. The vast array of cases constitutes a rich field for future study. Furthermore, we can prove that the general question of whether a population on a graph is vulnerable to invasion under frequency-dependent selection is NP (nondeterministic polynomial time)-hard.

The super-star possesses powerful amplifying properties in the case of games as well. For instance, in the positive symmetric orientation, the fixation probability for large N of a single A mutant is given by equation (1) with $r = (b/d)(b/c)^{K-1}$. For a super-star with large K, this r value diverges as long as $b > c$. Thus, even a dominated strategy ($a < c$ and $b < d$) satisfying $b > c$ will expand from a single mutant to conquer the entire super-star with a probability that can be made arbitrarily close to 1. The guaranteed fixation of this broad class of dominated strategies is a unique feature of evolutionary game theory on graphs: without structure, all dominated strategies die out. Similar results hold for the super-star in other orientations.

Evolutionary graph theory has many fascinating applications. Ecological habitats of species are neither regular spatial lattices nor simple two-dimensional surfaces, as is usually assumed[20,21], but contain locations that differ in their connectivity. In this respect, our results for scale-free graphs are very suggestive. Source and sink populations have the effect of suppressing selection, like one-rooted graphs[22,23].

Another application is somatic evolution within multicellular organisms. For example, the hematopoietic system constitutes an evolutionary graph with a suppressive hierarchical organization; stem cells produce precursors which generate differentiated cells[24]. We expect tissues of long-lived multicellular organisms to be organized so as to suppress the somatic evolution that leads to cancer. Star structures can also be instantiated by populations of differentiating cells. For example, a stem cell in the centre generates differentiated cells, whose offspring either differentiate further, or revert back to stem cells. Such amplifiers of selection could be used in various developmental processes and also in the affinity maturation of the immune response.

Human organizations have complicated network structures[25–27]. Evolutionary graph theory offers an appropriate tool to study selection on such networks. We can ask, for example, which networks are well suited to ensure the spread of favourable concepts. If a company is strictly one-rooted, then only those ideas that originate from the root will prevail (the CEO). A selection amplifier, like a star structure or a scale-free network, will enhance the spread of favourable ideas arising from any one individual. Notably, scientific collaboration graphs tend to be scale-free[28].

We have sketched the very beginnings of evolutionary graph theory by studying the fixation probability of newly arising mutants. For constant selection, graphs can dramatically affect the balance between drift and selection. For frequency-dependent selection, graphs can redirect the process of selection itself.

Many more questions lie ahead. What is the maximum mutation rate compatible with adaptation on graphs? How does sexual reproduction affect evolution on graphs? What are the timescales associated with fixation, and how do they lead to coexistence in ecological settings[29,30]? Furthermore, how does the graph itself change as a consequence of evolutionary dynamics[31]? Coupled with the present work, such studies will make increasingly clear the extent to which population structure affects the dynamics of evolution. □

Received 10 September; accepted 16 November 2004; doi:10.1038/nature03204.

1. Liggett, T. M. *Stochastic Interacting Systems: Contact, Voter and Exclusion Processes* (Springer, Berlin, 1999).
2. Durrett, R. & Levin, S. A. The importance of being discrete (and spatial). *Theor. Popul. Biol.* **46,** 363–394 (1994).
3. Moran, P. A. P. Random processes in genetics. *Proc. Camb. Phil. Soc.* **54,** 60–71 (1958).
4. Durrett, R. A. *Lecture Notes on Particle Systems & Percolation* (Wadsworth & Brooks/Cole Advanced Books & Software, Pacific Grove, 1988).
5. Erdös, P. & Renyi, A. On the evolution of random graphs. *Publ. Math. Inst. Hungarian Acad. Sci.* **5,** 17–61 (1960).
6. Barabasi, A. & Albert, R. Emergence of scaling in random networks. *Science* **286,** 509–512 (1999).
7. Nagylaki, T. & Lucier, B. Numerical analysis of random drift in a cline. *Genetics* **94,** 497–517 (1980).
8. Wright, S. Evolution in Mendelian populations. *Genetics* **16,** 97–159 (1931).
9. Wright, S. The roles of mutation, inbreeding, crossbreeding and selection in evolution. *Proc. 6th Int. Congr. Genet.* **1,** 356–366 (1932).
10. Fisher, R. A. & Ford, E. B. The "Sewall Wright Effect". *Heredity* **4,** 117–119 (1950).
11. Barton, N. The probability of fixation of a favoured allele in a subdivided population. *Genet. Res.* **62,** 149–158 (1993).
12. Whitlock, M. Fixation probability and time in subdivided populations. *Genetics* **164,** 767–779 (2003).
13. Nowak, M. A. & May, R. M. The spatial dilemmas of evolution. *Int. J. Bifurcation Chaos* **3,** 35–78 (1993).
14. Hauert, C. & Doebeli, M. Spatial structure often inhibits the evolution of cooperation in the snowdrift game. *Nature* **428,** 643–646 (2004).
15. Hofbauer, J. & Sigmund, K. *Evolutionary Games and Population Dynamics* (Cambridge Univ. Press, Cambridge, 1998).
16. Maruyama, T. Effective number of alleles in a subdivided population. *Theor. Popul. Biol.* **1,** 273–306 (1970).
17. Slatkin, M. Fixation probabilities and fixation times in a subdivided population. *Evolution* **35,** 477–488 (1981).
18. Ebel, H. & Bornholdt, S. Coevolutionary games on networks. *Phys. Rev. E.* **66,** 056118 (2002).
19. Abramson, G. & Kuperman, M. Social games in a social network. *Phys. Rev. E.* **63,** 030901(R) (2001).
20. Tilman, D. & Karieva, P. (eds) *Spatial Ecology: The Role of Space in Population Dynamics and Interspecific Interactions* (Monographs in Population Biology, Princeton Univ. Press, Princeton, 1997).
21. Neuhauser, C. Mathematical challenges in spatial ecology. *Not. AMS* **48,** 1304–1314 (2001).
22. Pulliam, H. R. Sources, sinks, and population regulation. *Am. Nat.* **132,** 652–661 (1988).
23. Hassell, M. P., Comins, H. N. & May, R. M. Species coexistence and self-organizing spatial dynamics. *Nature* **370,** 290–292 (1994).
24. Reya, T., Morrison, S. J., Clarke, M. & Weissman, I. L. Stem cells, cancer, and cancer stem cells. *Nature* **414,** 105–111 (2001).
25. Skyrms, B. & Pemantle, R. A dynamic model of social network formation. *Proc. Nat. Acad. Sci. USA* **97,** 9340–9346 (2000).
26. Jackson, M. O. & Watts, A. On the formation of interaction networks in social coordination games. *Games Econ. Behav.* **41,** 265–291 (2002).
27. Asavathiratham, C., Roy, S., Lesieutre, B. & Verghese, G. The influence model. *IEEE Control Syst. Mag.* **21,** 52–64 (2001).
28. Newman, M. E. J. The structure of scientific collaboration networks. *Proc. Natl Acad. Sci. USA* **98,** 404–409 (2001).
29. Boyd, S., Diaconis, P. & Xiao, L. Fastest mixing Markov chain on a graph. *SIAM Rev.* **46,** 667–689 (2004).
30. Nakamaru, M., Matsuda, H. & Iwasa, Y. The evolution of cooperation in a lattice-structured population. *J. Theor. Biol.* **184,** 65–81 (1997).
31. Bala, V. & Goyal, S. A noncooperative model of network formation. *Econometrica* **68,** 1181–1229 (2000).

Supplementary Information accompanies the paper on **www.nature.com/nature**.

Acknowledgements The Program for Evolutionary Dynamics is sponsored by J. Epstein. E.L. is supported by a National Defense Science and Engineering Graduate Fellowship. C.H. is grateful to the Swiss National Science Foundation. We are indebted to M. Brenner for many discussions.

Competing interests statement The authors declare that they have no competing financial interests.

Correspondence and requests for materials should be addressed to E.L. (erez@erez.com).

Supplementary Notes

Here we sketch the derivations of eq (1) for circulations and eq (2) for superstars. We give a brief discussion of complexity results for frequency-dependent selection and the computation underlying our results for directed cycles. We close with a discussion of our assumptions about mutation rate and the interpretations of fitness which these results can accommodate.

Evolution on graphs is a Markov process.

Let G be a graph whose adjacency matrix is given by W. Let $\mathbf{P} \subset \mathbf{V}$ be the set of vertices occupied by a mutant at some iteration. $\mathbf{P}$ represents a state of the typical Markov chain E_G which arises on an evolutionary graph. Analogously, the states $P = \{1, 2, ...N\}$ are the typical states of the Moran process M.

(For two types of individuals, the states of the explicit Markov chain E_G are the 2^n possible arrangements of mutants on the graph. The transition probability between two states $\mathbf{P}$, $\mathbf{P'}$ is 0 unless $\mid \mathbf{P} \backslash \mathbf{P'} \mid = 1$ or vice versa. Otherwise, if $\mathbf{P} \backslash \mathbf{P'} = v^*$, then the probability of a transition from $\mathbf{P}$ to $\mathbf{P'}$ is

$$\frac{\sum_{v \in G \backslash \mathbf{P}} w(v, v^*)}{N + \mid \mathbf{P} \mid (r-1)}$$

where the numerator is the sum of the weights of edges entering v* from vertices outside $\mathbf{P}$. Similarly, the probability of a transition from $\mathbf{P'}$ to $\mathbf{P}$ is

$$\frac{\sum_{v \in \mathbf{P'}} w(v, v^*)}{N + \mid \mathbf{P'} \mid (r-1)}$$

In practice, the resulting matrix is large and not very sparse. Consequently, it can be difficult to work with directly, and we will not revisit it in the course of these notes.)

We now define the notion of ρ-equivalency.

Definition 1. A graph G is ρ-equivalent to the Moran process if the cardinality map f($\mathbf{P}$) = $\mid \mathbf{P} \mid$ from the states of E_G to the states of M preserves the ultimate fixation probabilities of the states. Equivalently, we need

$$\rho(r, G, P, N) = \frac{1 - 1/r^P}{1 - 1/r^N}$$

where $\rho(r, G, P, N)$ is the probability that a mutant of fitness r on a graph G, given any initial population of size P, eventually reaches the fixation population of N. (Note that this function is often undefined: on most graphs, different initial conditions with the same number of mutants have different fixation probabilities.)

Note that eq (1) is obtained in the case $P = 1$.
This shows that the requirement of preserving fixation probabilities leads inevitably to the preservation of transition probabilities between all the states. In particular, it means that the population size on G, $\mid \mathbf{P} \mid$, performs a random walk with a forward bias of r, e.g., where the probability of a forward step is $r/(r + 1)$.

Evolution on circulations is equivalent to the Moran process.

We now provide a necessary and sufficient condition for ρ-equivalence to the Moran process for the case of an arbitrary weighted digraph G. The isothermal theorem for stochastic matrices is obtained as a corollary. First we state the definition of a circulation.

Definition 2. The matrix W defines a circulation $\leftrightarrow$

$$\forall i, \sum_j w_{ij} = \sum_j w_{ji}$$

This is precisely the statement that the graph G_W satisfies

$$\forall v \in G, w_o(v) = w_i(v)$$

where w_o and w_i represent the sum of the weights entering and leaving v.

It is now possible to state and prove our first result.

Theorem 1. *(Circulation Theorem.) The following are equivalent:*
(1) G is a circulation.
(2) $\mid \mathbf{P} \mid$ performs a random walk with forward bias r and absorbing states at $\{0, N\}$.
(3) G is ρ-equivalent to the Moran process
(4)

$$\rho(r, G, P, P') = \frac{1 - 1/r^P}{1 - 1/r^{P'}}$$

where $\rho(r, G, P, P')$ is the probability that a mutant of fitness r on a graph G given any initial condition with P mutants eventually reaches a mutant population of P'.

Proof. We show that (1) $\rightarrow$ (2) $\rightarrow$ (3) $\rightarrow$ (4) $\rightarrow$ (1).
To see that (1) $\rightarrow$ (2), let $\delta_+(\mathbf{P})$ (resp. $\delta_-(\mathbf{P})$) be the probability that the mutant population in a given state increases (resp. decreases), where $\mathbf{P} \subset \mathbf{V}$ is just the set of vertices occupied by a mutant, corresponding to the present state. The mutant population size will only change if the edge selected in the next round is a member of an edge cut of $\mathbf{P}$, e.g., the head is in $\mathbf{P}$ and the tail is not, or vice-versa.
The probability of a population increase in the next round, $\delta_+(\mathbf{P})$, is therefore just the weight of all the edges leaving $\mathbf{P}$, adjusted by the fitness of the mutant r. Thus

$$\delta_+(\mathbf{P}) = \frac{w_o(\mathbf{P})r}{w_o(\mathbf{P})r + w_i(\mathbf{P})}$$

where w_o and w_i represent the sum of the weights entering and leaving a vertex set $\mathbf{P}$. Similarly,

$$\delta_-(\mathbf{P}) = \frac{w_i(\mathbf{P})}{w_o(\mathbf{P})r + w_i(\mathbf{P})}$$

Dividing, we easily obtain

$$\frac{\delta_+(\mathbf{P})}{\delta_-(\mathbf{P})} = r\frac{w_o(\mathbf{P})}{w_i(\mathbf{P})}$$

We may also observe that

$$w_o(\mathbf{P}) - w_i(\mathbf{P}) = (\sum_{v \in \mathbf{P}} w_o(v) - \sum_{e|e_1,e_2 \in \mathbf{P}} w(e)) - (\sum_{v \in \mathbf{P}} w_i(v) - \sum_{e|e_1,e_2 \in \mathbf{P}} w(e))$$
$$= (\sum_{v \in \mathbf{P}} w_o(v) - \sum_{v \in \mathbf{P}} w_i(v))$$

where the second and fourth sums in the latter equality are over edges whose two endpoints are in P. Since this vanishes when G is a circulation, we find that on a circulation

$$\forall \mathbf{P} \subset \mathbf{V}, w_o(\mathbf{P}) = w_i(\mathbf{P})$$

and therefore

$$\frac{\delta_+(\mathbf{P})}{\delta_-(\mathbf{P})} = r$$

for all $\mathbf{P}$.

Thus the population is simply performing a random walk with forward bias r as desired, yielding (1) $\rightarrow$ (2).

(2) $\rightarrow$ (3) follows immediately from the theory of random walks.

It is easy to see that (3) $\rightarrow$ (4) by conditional probabilities. We know that

$$\forall P' \geq P, \rho(r, G, P, N) = \rho(r, G, P, P') * \rho(r, G, P', N)$$

Therefore

$$\forall P' \geq P, \rho(r, G, P, P') = \frac{\rho(r, G, P, N)}{\rho(r, G, P', N)}$$
$$= \frac{1 - 1/r^P}{1 - 1/r^N} (\frac{1 - 1/r^{P'}}{1 - 1/r^N})^{-1}$$
$$= \frac{1 - 1/r^P}{1 - 1/r^{P'}}$$

which is the desired result.

To complete the proof, we show that (4) $\rightarrow$ (1). By (4), we know

$$\rho(1,2,G,r) = \frac{1-\frac{1}{r}}{1-\frac{1}{r^2}} = \frac{r}{r+1}$$

But this is only satisfied for all populations of size 1 if we have

$$\forall v, \frac{\delta_+(v)}{\delta_-(v} = r$$

As we saw above, this implies that

$$\forall v, w_o(v) = w_i(v)$$

which demonstrates that G must be a circulation and completes the proof. □

The isothermal result is just a corollary.

Theorem 2. *(Isothermal Theorem.) G is ρ-equivalent to the Moran process ⇔ G is isothermal, e.g., W is doubly-stochastic.*

Superstars are arbitrarily strong amplifiers of natural selection.

We now sketch the derivation of the amplifier theorem for superstars, denoted $S^K_{L,M}$, where K is the amplification factor, L the number of leaves, and M the number of vertices in the reservoir of each leaf. First we must precisely define these objects.

Definition 3. The Super-star $S^K_{L,M}$ consists of a central vertex v_{center} surrounded by L leaves. Leaf ℓ contains M reservoir vertices, $r_{\ell,m}$ and K-2 ordered chain vertices $c_{\ell,1}$ through $c_{\ell,K-2}$. All directed edges of the form ($r_{\ell,m}$, $c_{\ell,1}$), ($c_{\ell,w}$,$c_{\ell,w+1}$), ($c_{\ell,K+2}$,v_{center}), and (v_{center}, $r_{\ell,m}$) exist and no others. In the case $K = 2$, the edges are of the form ($r_{\ell,m}$, v_{center}), and (v_{center}, $r_{\ell,m}$). Illustrations for $K = 2$ and $K = 3$ are given in Fig 3. The weight of an edge (i,j) is given by $1/d_o(i)$, where d_o is the out-degree.

Now we may move on to the theorem.

Theorem 3. *(Super-star Theorem.) As the number and size of the leaves grows large, the fixation probability of a mutant of fitness r on a super-star of parameter K converges toward the behavior of a mutant of fitness r^K on a circulation:*

$$\lim_{L,M\to\infty} \rho(S^K_{L,M}) \to \frac{1-1/r^K}{1-1/r^{KN}}$$

Proof. (Sketch) The proof has several steps.

First we observe that for large M, the mutant is overwhelmingly likely to appear outside the center or the chain vertices.

Now we show that if the density of mutants in an upstream population is d, then the probability that an individual in a population immediately downstream will be a mutant at any given time is $\frac{dr}{1+d(r-1)}$. In general, if we have η populations, one upstream of the other, the first of which has mutant probability density d=d(1), we obtain the following probability density for the ν^{th} population

$$d(\nu) = \frac{dr^\nu}{1+d(r^\nu-1)}$$

The result follows inductively from the observation that

$$d(j+1) = \frac{\frac{dr^j}{1+d(r^j-1)}r}{1+\frac{dr^j}{1+d(r^j-1)}(r-1)}$$

$$= \frac{dr^{j+1}}{1+d(r^{j+1}-1)}$$

For the super-star, this result is precise as we move inward from the leaf vertices along the chain leading into the central vertex, where derivation of an analogous result is necessary. Here we require careful bounding of error terms, and allowing L to go off to the infinite limit. This is in order to ensure that 'feedback' is sufficiently attenuated: otherwise, during the time required for information about upstream density to propagate to the central vertex, the upstream population will have already changed too significantly. In this latter regime, 'memory' effects can give the resident a very

significant advantage: the initial mutant has died before the central vertex is fully affected by its presence. For sufficiently many leaves feedback is irrelevant to fixation. In the relevant regime we establish that the central vertex is a mutant with probability

$$d(K-1) = \frac{dr^{K-1}}{1 + d(r^{K-1} - 1)}$$

Our result follows by noting that the probability of an increase in the number of mutant leaf vertices during a given round is very nearly

$$\frac{r}{N + P(r-1)} \frac{dr^{K-1}}{1 + d(r^{K-1} - 1)} (1 - d)$$

and the probability of a decrease is

$$\frac{1}{N + P(r-1)} \frac{1 - d}{1 + d(r^{K-1} - 1)} d$$

Dividing, all the terms cancel but an r^K in the numerator. Thus the mutant population in the leaves performs a random walk with a forward bias of r^K until fixation is guaranteed or the strain dies out. □

In the spirit of this result, we may define an amplification factor for any graph G with N vertices as the value of K for which $\rho(G) = \frac{1-1/r^K}{1-1/r^{KN}}$. We have seen above that a superstar of parameter K has an amplification factor of K as N grows large.

The fixation problem for frequency-dependent evolution on graphs is at least as hard as NP.

NP-hard problems arise naturally in the study of frequency-dependent selection on graphs. Let us consider the general case of some finite number of types; a state of the graph is a partition of its vertices among the types, or a coloring. Given a graph G and an initial state I, let VULNERABILITY be the decision problem of whether, given a graph G, an initial state I, a small constant ϵ, and a desired winning type T, fewer than w individuals can mutate to T so as to ensure fixation of the graph by

T with probability at least 1-ϵ. By reduction from the Boolean Circuit Satisfiability problem, it can be shown the VULNERABILITY is NP-hard. We omit the details of the proof here.

Frequency-dependent evolution on graphs leads to a multiplicity of invasion criteria.

The following computation establishes our observations about directed cycles.

Proposition 4. *(Fixation on Directed Cycles.) For large N, the directed cycle favors mutants where b>c (resp. a>d, a>c, b>d) in the positive symmetric (resp. negative symmetric, positive antisymmetric, negative antisymmetric) orientations.*

Proof. (Sketch) For the positive symmetric case, we obtain eq (1) with $r = b/c$ as a straightforward instance of gambler's ruin with bias b/c. In the other three orientations, a bit more work is required to account for the case where the patch is of size 1 or size of N-1. In the negative symmetric and positive antisymmetric orientations, the mutant has an aberrant fitness of b for patch sizes of exactly 1 (near extinction). In both negative orientations, the resident has an aberrant fitness of c when the mutant patch is of size N-1 (near fixation). Thus we must do some work to ensure that these aberrations do not ultimately affect which types of mutants are favored on large cycles.
We must evaluate the following expression to obtain the fixation probability of the biased random walk:

$$\rho = \frac{1}{1 + \Sigma_{i=1}^{N-1} \Pi_{j=1}^{i} \frac{q_i}{p_i}}$$

The values of p_i and q_i represent probabilities of increase and decrease when the population is of size i. We obtain

$$\rho_{-s} = \frac{b(d-a)}{bd - ab - ad + (d/a)^{N-2}(ad + cd - ac)}$$

$$\rho_{+a} = \frac{b(c-a)}{bc - ab - ac + (c/a)^{N-2}(c^2)}$$

$$\rho_{-a} = \frac{b(d-b)}{-b^2 + (d/b)^{N-2}(bd + cd - bc)}$$

for the negative symmetric, positive antisymmetric, and negative antisymmetric cases. For large N, these expressions are smaller than the neutral fixation probability 1/N if d/a (resp. c/a, d/b) is greater than one; if it is less than 1, the fixation probabilities converge to

$$\rho_{-s} = \frac{b(a-d)}{b(a-d) + ad}$$

$$\rho_{+a} = \frac{b(a-c)}{b(a-c) + ac}$$

$$\rho_{-a} = \frac{b(b-d)}{b^2}$$

and the mutant is strongly favored over the neutral case. □

Results hold if fertility and mortality are independent Poisson processes.

Finally, we will make some remarks about our assumptions regarding mutation rate and the meaning of our fitness values.

It is generally the case that suppressing either selection or drift, and in particular the latter, is time intensive. Good amplifiers get arbitrarily large as $\rho \to 1$ or 0, and have increasingly significant bottlenecks. Thus, fixation times get extremely long the more effectively drift is suppressed. However, since we are working in the limit where mutations are very rare, this timescale can be ignored. The rate of evolution reduces to the product of population size, mutation rate, and fixation probability.

In our discussions, we have treated fitness as a measure of reproductive fertility. But a range of frequency-independent interpretations of fitness obtain identical results. If

instead of choosing an individual to reproduce in each round with probability proportional to fitness, we choose an individual to die with probability inversely proportional to fitness, and then replace it with a randomly-chosen upstream neighbor, the ρ values obtained are identical. Put another way, as long as reproduction (leading to death of a neighbor by overcrowding) and mortality (leading to the reproduction of a neighbor that fills the void) are independent Poisson processes, our results will hold.